



Influence of supported-metal characteristics on deNO_x catalytic activity over Pt/CeO₂

Masahiro Itoh^a, Makoto Saito^a, Masahiko Takehara^a, Koji Motoki^a, Jun Iwamoto^b, Ken-ichi Machida^{a,*}

^a Center for Advanced Science and Innovation, Osaka University, 2-1 Yamadaoka, Suita, Osaka 565-0871, Japan

^b Honda R&D Co., Ltd., Automobile R&D Center, 4630 Shimotakanezawa, Haga-machi, Haga-gun, Tochigi 321-3393, Japan

ARTICLE INFO

Article history:

Received 15 October 2008

Received in revised form 4 February 2009

Accepted 4 February 2009

Available online 13 February 2009

Keywords:

H₂-SCR

deNO_x

Solvothermal

Ceria supported Pt catalyst

Metal–support interaction

ABSTRACT

Fine Pt particles were loaded on the CeO₂ supports with various specific surface areas by an incipient wetness method or a solvothermal one, and their catalytic properties for the NO_x reduction by hydrogen were tested. The Pt/CeO₂ catalysts prepared by the solvothermal method provided higher activity than those by the impregnation one when using the CeO₂ support with high surface area. Each CeO₂ supports and Pt particles prepared by the solvothermal method did not show the good catalytic activity singly. However the catalysts obtained by physically mixing Pt particles with the CeO₂ supports gave excellent NO_x conversion of ca. 80% with relative high N₂ selectivity (75%).

© 2009 Elsevier B.V. All rights reserved.

1. Introduction

NO and NO₂ (referred to as NO_x) emitted from mobile and stationary internal combustion is one of the most closely monitored categories of pollutants, since NO_x leads photochemical smog and acid rain. To meet their strict emission regulations, selective catalytic reduction (SCR) for NO_x by using NH₃ (including urea system), CO, hydrocarbon, or H₂ as a reducing agent has been extensively investigated [1–8]. Among them, the H₂-SCR has an advantage on high conversion of NO_x reduction at relatively low temperature under excess oxygen condition such as lean fuel/air ratio combustion. Additionally, hydrogen can be generated on board by controlling engine emission or using Reforming and exhaust gas recirculation (REGR) [9]. So the H₂-SCR system has been considered as a candidate of NO_x control technology in place of the present NH₃ (or urea)-SCR method. Such H₂-SCR for NO_x, however, tends to produce more N₂O causing greenhouse warming rather than N₂ during the reaction. The N₂ selectivity cannot be improved by changing precious metal loadings or H₂ concentration in the feed gas, but is affected by acidity/basicity character of the oxides used as a support [10]. In our recent work, H₂-SCR activity for NO_x over the platinum supported rare earth oxide catalysts has been investigated to elucidate the influence of the solid acidity/basicity on

the N₂ selectivity and NO_x conversion, because rare earth oxides change their acidity/basicity by decreasing their ionic radii accompanied with lanthanide contraction [11]. Although almost all the catalysts did not provide the good catalytic activity, only Pt/CeO₂ showed the high NO_x conversion at around 373 K. NH₃ temperature-programmed desorption (TPD) profiles for the Pt/rare earth oxide catalysts revealed that their solid acidity is not drastically different, suggesting that the specific interaction between Pt and CeO₂ influences the NO_x reduction activity, rather than solid acidity.

In this study, two different Pt loading techniques such as an incipient wetness method and a solvothermal one, where the latter is effective to prepare the Pt metal with high crystallinity confirmed from our previous work [12], were applied to the CeO₂ supports with different specific surface area to modify the metal/support interface circumstance. Their catalytic properties for NO_x reduction were discussed from the viewpoint of metal–support interaction.

2. Experimental

Two types of CeO₂ supports having high and low specific surface area were used in this study. For the incipient wetness method, respective water absorption amounts for these CeO₂ supports were measured before the impregnation procedure. Then the CeO₂ powders were added to the corresponding volume of Pt(NO₃)₂ aqueous solutions with setting Pt loading of 1 wt% and mixed thoroughly to get slurries. The resulting slurries were dried at 393 K overnight and then calcined at 873 K for 2 h in air. For the solvothermal method,

* Corresponding author. Tel.: +81 6 6879 4209; fax: +81 6 6879 4209.

E-mail address: machida@casi.osaka-u.ac.jp (K.-i. Machida).

appropriate amounts of the CeO_2 powders and the $\text{Pt}(\text{NO}_3)_2$ aqueous solution were added to 80 ml of isopropyl alcohol in a test tube, and the test tube was placed in a 100 ml autoclave vessel. Subsequently the sealed vessel was kept at 573 K for 12 h to conduct a Pt deposition reaction completely. In fact, the solution color changed from yellow to transparent after the reaction, indicating the above deposition almost fully proceeded. After cooling to room temperature, the products were collected by a centrifuge and repeatedly washed with acetone. The resultant powders were dried at 323 K overnight in air, and then calcined at 873 K for 2 h in air. For convenient, the catalysts are labeled as follows: the catalysts prepared by the incipient wetness method with using low and high specific surface area CeO_2 are represented as IW-Pt/L- CeO_2 and IW-Pt/H- CeO_2 , respectively. In a similar way, the catalysts prepared by the solvothermal method are represented as ST-Pt/L- CeO_2 and ST-Pt/H- CeO_2 .

Nitrogen adsorption isotherm was measured at 77 K to evaluate the specific surface area using Brunauer, Emmett, and Teller's (BET) equation. CO chemisorption was carried out by a pulse technique at room temperature to determine the Pt metal dispersion [13]. CO_2 TPD experiments were carried out to estimate the solid basicity from the desorption temperature by using a gas chromatograph equipped with TCD. The sample surface area contacting CO_2 roughly set to 10 m^2 for all specimens by adjusting their weight to enhance a signal/noise ratio. Temperature-programmed reaction (TPR) experiments were performed in order to investigate the reaction between hydrogen and NO_x species adsorbed on a surface of the catalysts. Before starting the TPR experiments, NO (0.1 vol%) and O_2 (10 vol%) mixed gases balanced with He (total flow rate of 30 ml min^{-1}) are passed at 473 K. The effluent gas was analyzed by an on-line mass spectrometer (Pfeiffer Vacuum, PrismaPlus)

with flowing a reactant gas stream (0.4 vol% H_2 and balanced He with a total flow rate of 30 mL min^{-1}) at 323–623 K. Further physical properties were characterized by X-ray diffraction with Cu-K α radiation (RIGAKU, RINT2200), transmission electron microscopy (JEOL, JEM-2010F), and scanning electron microscopy (HITACHI, S-3000H). Catalytic testing was performed at atmospheric pressure in a conventional fixed-bed quartz reactor. Gas mixtures of 0.1 vol% NO, 0.4 vol% H_2 , 10 vol% O_2 , and balanced with N_2 were fed to the catalyst sample with 0.15 g ($\text{W/F} = 0.3 \text{ g s mL}^{-1}$) placed in the reactor tube. The effluent from the reactor was analyzed by an online FT-IR spectrometer with a gas cell (PerkinElmer, Spectrum 2000). Spectra were collected by scanning five times from 1000 cm^{-1} to 4000 cm^{-1} at resolution of 0.5 cm^{-1} . Concentrations of NO, NO_2 , and N_2O were determined from their calibration curves by integrating the peak area at respective 1911, 1586, and 2214 cm^{-1} . No ammonia formation was observed in this study. The N_2 production was evaluated by subtracting NO, NO_2 , and N_2O concentrations of outlet gas from the inlet NO concentration. Diffuse reflectance infrared Fourier transform spectroscopy (DRIFTS) was performed by using the above spectrometer with a temperature controllable diffuse reflectance reaction cell to observe adsorption chemical species *in situ*.

3. Results and discussion

Fig. 1 shows the NO_x conversion, N_2 selectivity, and N_2O selectivity on the Pt/ CeO_2 catalysts prepared in this study as a function of the reaction temperatures. ST-Pt/H- CeO_2 showed the good NO_x conversion with the N_2 selectivity of ca. 40%. On the contrary, the NO_x reduction activity for IW-Pt/H- CeO_2 was poor as reported by Machida et al. [14] The BET surface area values on the respective

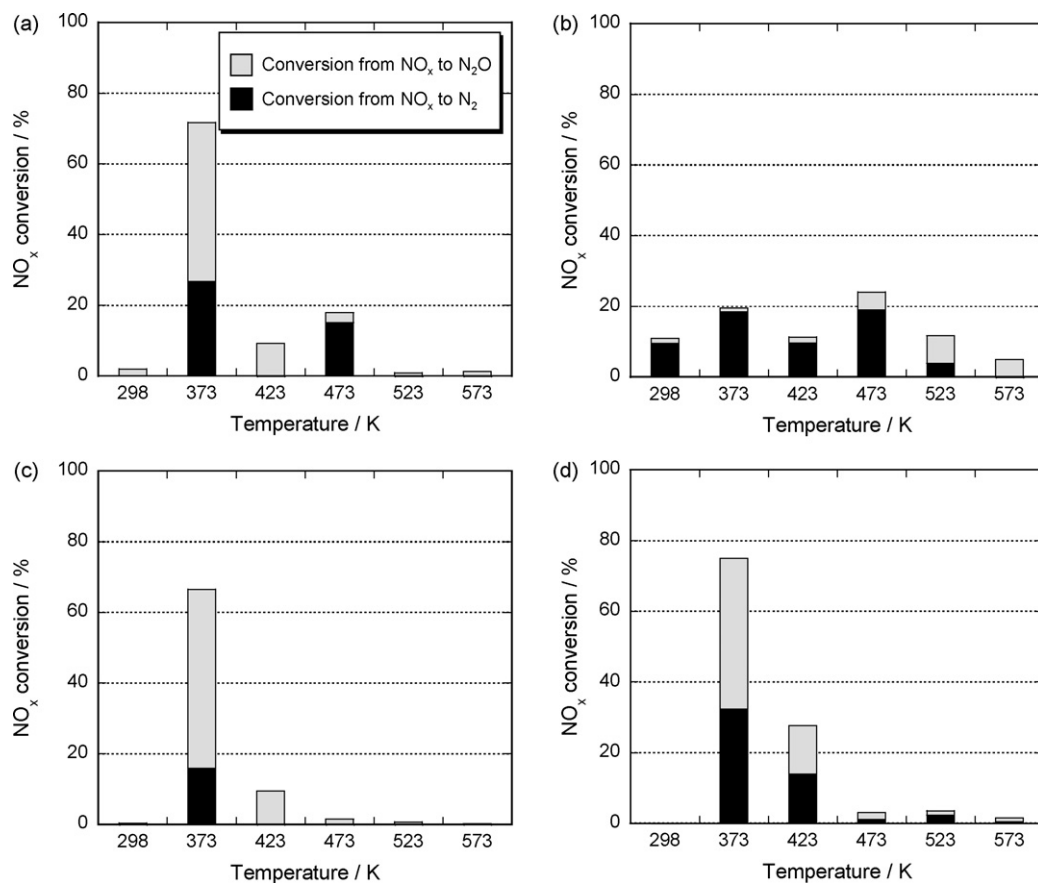


Fig. 1. NO_x conversion and selectivity as a function of temperature observed on (a) ST-Pt/H- CeO_2 , (b) IW-Pt/H- CeO_2 , (c) ST-Pt/L- CeO_2 , and (d) IW-Pt/L- CeO_2 . Grey and black bars represent the N_2O and N_2 selectivity, respectively.

Table 1
Characteristics of the Pt/CeO₂ catalysts.

Catalysts	Surface area [m ² /g]	CO adsorption [μmol/g]	Dispersion [%] ^a	Pt particle size [nm]
ST-Pt/H-CeO ₂	119	34	67	1.7
IW-Pt/H-CeO ₂	135	38	74	1.5
ST-Pt/L-CeO ₂	5	1.4	3	41
IW-Pt/L-CeO ₂	9	8.3	16	6.9

^a Calculated as CO:Pt = 1:1.

ST-Pt/H-CeO₂ and IW-Pt/H-CeO₂ were 119 and 135 m²/g as summarized in Table 1. The Pt metal dispersion for IW-Pt/H-CeO₂ (74%) was slightly higher than that for ST-Pt/H-CeO₂ (67%). The Pt particle size directly observed by the TEM dark field images for ST-Pt/H-CeO₂ and IW-Pt/H-CeO₂ were well consistent with the CO chemisorption results, and their morphology were analogously spherical as shown in Fig. 2. On the other hand, the NO_x conversion activity on IW-Pt/L-CeO₂ was considerably improved by decreasing surface area of the CeO₂ support as shown in Fig. 1(d). In using the CeO₂ support with low surface area, the NO_x reduction properties were almost same for each catalyst prepared by the solvothermal and incipient wetness methods, though their Pt metal dispersion greatly varied as listed in Table 1. Fig. 3 shows the CO₂-TPD profiles obtained on the CeO₂ supports with high and low surface area. Both catalysts had peaks around 500 K and 700 K, which were derived from weak and moderate base sites, respectively [15], suggesting that they had the almost same solid base strength regardless of their surface area values. The results of CO chemisorption, TEM observation, and CO₂-TPD indicate that the NO_x reduction activity over the

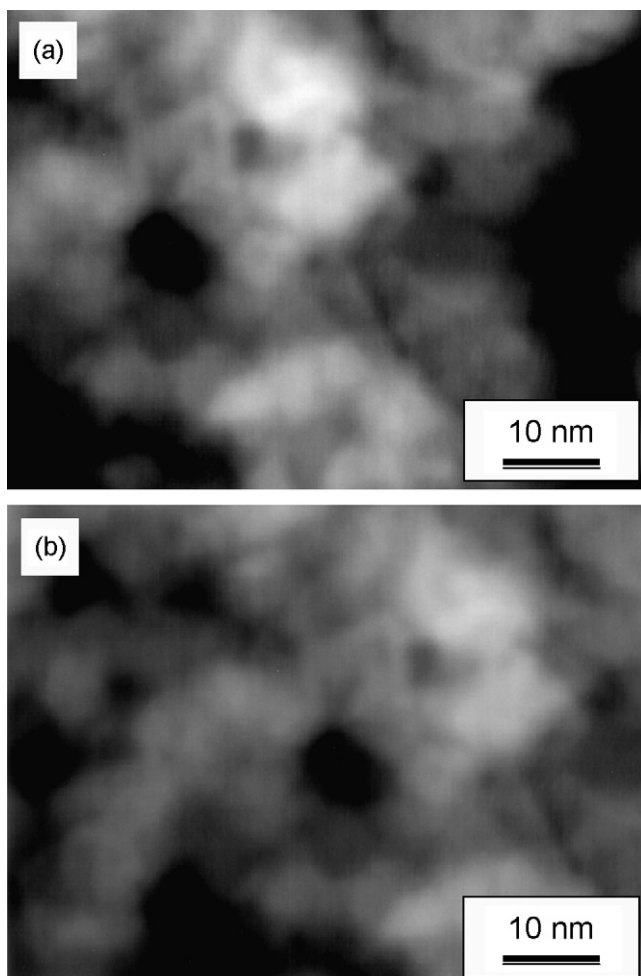


Fig. 2. TEM dark field images observed on (a) ST-Pt/H-CeO₂ and (b) IW-Pt/H-CeO₂.

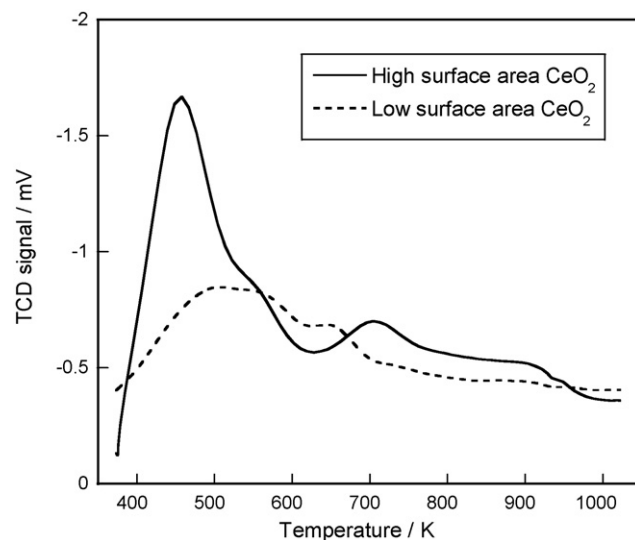


Fig. 3. CO₂ temperature-programmed desorption profile on the CeO₂ support with high surface area (solid line) and low surface area (dashed line).

Pt/CeO₂ catalysts was significantly affected by the metal–support interaction. The IW-Pt/H-CeO₂ catalysts, which had the largest contact area between Pt and CeO₂ in the catalysts prepared in this study, resulted in the low NO_x conversion. The suitable interaction is necessary to induce the good catalytic activity. The solvothermal method is probably effective to obtain such weak metal–support contact force, because nucleus growth rather than crystal nucleation is dominant during the solvothermal Pt deposition, resulting in decrease of Pt–CeO₂ bond leakage in the interface. In fact, the obvious diffraction peaks derived from face centered cubic symmetry of Pt metal in addition to the peaks from the CeO₂ phase were detected only on the XRD pattern of ST-Pt/L-CeO₂ as shown

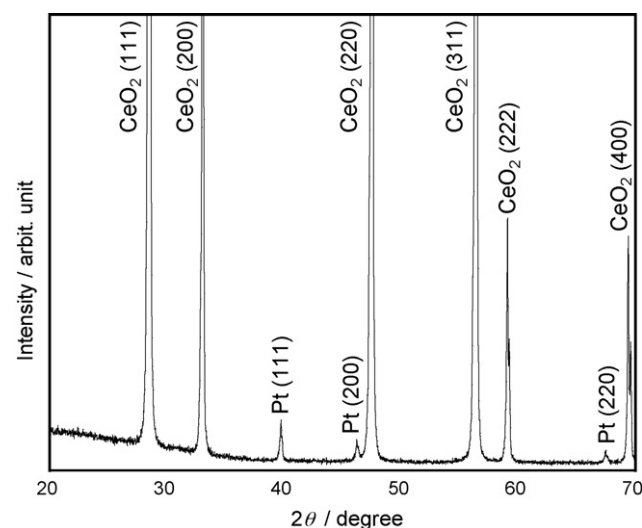


Fig. 4. XRD pattern obtained on ST-Pt/L-CeO₂ with Cu-Kα radiation.

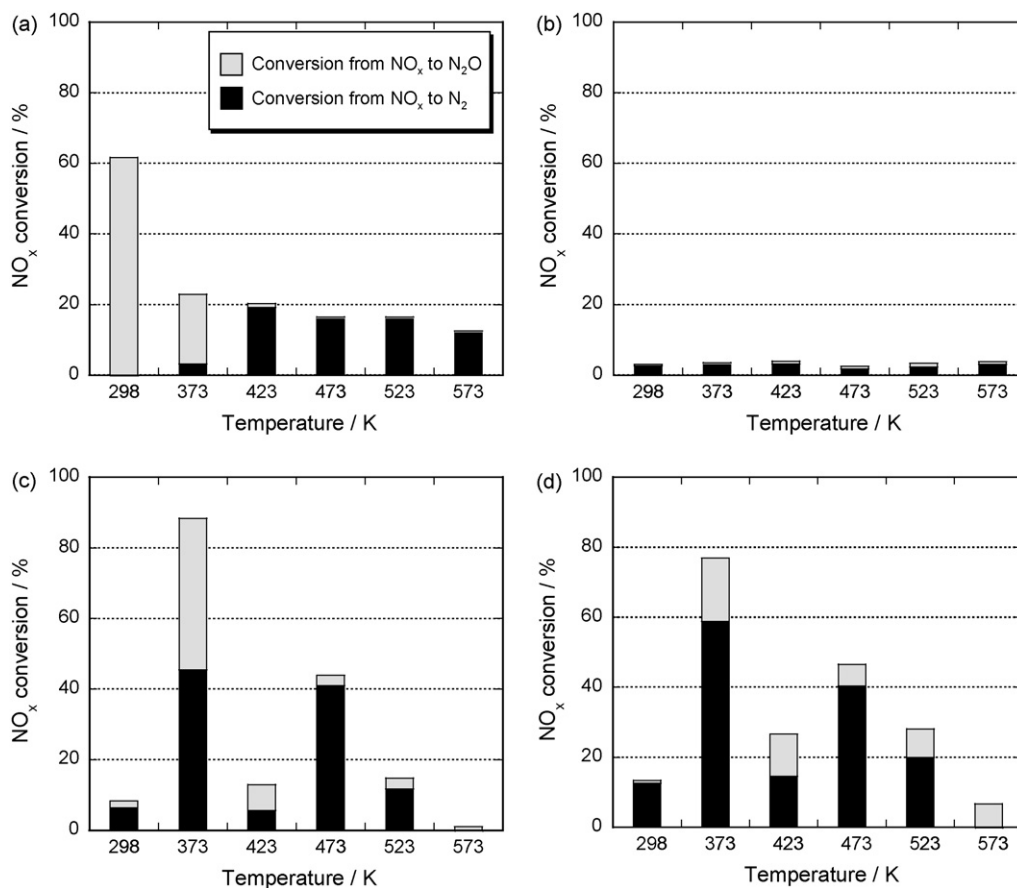


Fig. 5. NO_x conversion and selectivity as a function of temperature observed on (a) the Pt metal particles prepared by the solvothermal method, (b) the sole CeO₂ with high surface area, (c) the catalyst prepared by physically mixing (a) and (b), and (d) the catalyst prepared by mixing the Pt metal particles (reflux method) with (b). Grey and black bars represent the N₂O and N₂ selectivity, respectively.

in Fig. 4. Formation of the Pt particles with a several dozen nm was also confirmed from the CO chemisorption measurement (Table 1) and the direct TEM observation (not shown).

To investigate the reaction mechanism on the present Pt/CeO₂ catalysts, individual NO_x reduction activity on the sole Pt metal or CeO₂ support with high surface area was tested as shown in Fig. 5. The Pt metal particles were prepared by the solvothermal method in a similar manner mentioned above without adding the CeO₂ support. In the case of the support absence, well-crystallized Pt particles with fcc symmetry was obtained and they formed in a spherical shape with a diameter of ca. 100 nm as shown in

Figs. 6(a) and 7 (curve a). The Pt metal catalyst possessed the high NO_x conversion only at room temperature, in addition with high N₂O selectivity. The NO_x reduction activity became less with increasing the reaction temperature, and most NO was converted to NO₂ above 373 K (not indicating NO₂ selectivity in Fig. 5). Fig. 8(a) shows the DRIFT spectrum on the Pt metal catalyst at 373 K. No adsorbed species related nitrogen oxide was observed and symmetrical transmission peaks assigned to gaseous H₂O were observed at around 1300–1800 cm⁻¹. H₂ wastes by reacting with excess O₂ and cannot effectively work as a reducer for NO_x. As expected, the CeO₂ support did not show the catalytic activity against NO_x

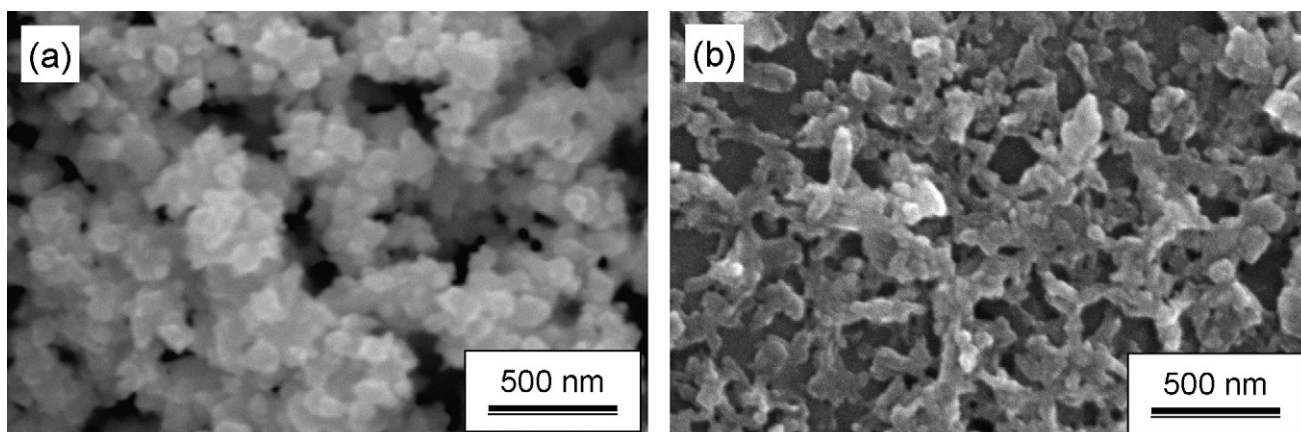


Fig. 6. SEM images of the Pt metal particles prepared by (a) solvothermal method and (b) reflux one.

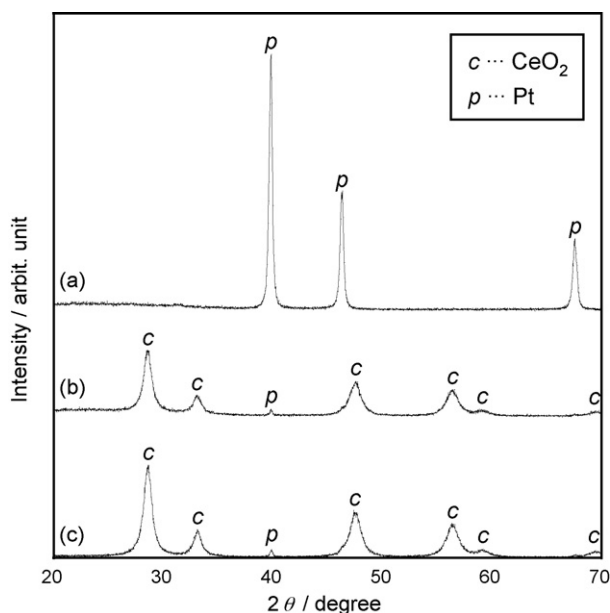


Fig. 7. XRD pattern obtained on the Pt metal particles prepared by the solvothermal method (curve a) as well as the Pt/CeO₂ mixed catalyst before (curve b) and after (curve c) the catalytic test.

reduction singly as shown in Fig. 5(b). It is well known that CeO₂ acts as a NO_x storage component besides one for oxygen [16]. The DRIFT spectrum for the CeO₂ support showed the formation of a strong transmission peak at 1180 cm⁻¹ assigned to nitrite as seen

in Fig. 8(b) [17]. The peak at 1430 cm⁻¹ are also derived from nitrite ion and the formation of nitrates was detected at 1300 cm⁻¹. Such strong adsorption of NO_x species retards further adsorption of other chemical reactants such as H₂ and O₂ and the poor NO_x conversion is resultantly attained.

In contrast, the catalyst prepared by physically mixing the above Pt metal particles (1 wt%) and CeO₂ support provided the good NO_x reduction activity with relative high N₂ selectivity of 50% at 373 K as shown in Fig. 5(c). Although deterioration of catalytic activity due to agglomeration should be considered for such mixed type catalysts, the deNO_x activity on the second test was almost same and the XRD patterns hardly changed before and after the first activity test as shown in Fig. 7 curves b and c. The serious agglomeration did not occur under the present reaction condition below 573 K. In addition, the NO_x conversion gave two maxima at 373 K and 473 K, suggesting there includes the different mechanism for NO_x reduction over this catalyst [18,19]. To our best knowledge, this is the first observation of such two conversion maxima on Pt-based catalysts having high affinity against H₂ and O₂. In the present catalyst system, Pt and CeO₂ have an important role each other; Pt adsorbs and dissociates chemical species such as H₂, O₂, NO, etc. and CeO₂ accumulates the NO_x species on its surface by proper solid basicity. It is considered that the NO_x reduction reaction proceeds on the interface between Pt and CeO₂. The H₂-TPR experiments bears out the above supposition as shown in Fig. 9. The NO_x species adsorbed on the sole Pt metal particle catalyst weakly reacts with hydrogen to generate trace amounts of N₂O (*m/z*=44). Meanwhile, various NO_x-reduced species such as N₂O, N₂ (*m/z*=28), and NH₃ (*m/z*=15 as NH⁺) were detected for the case of the Pt/CeO₂ mixed catalyst, suggesting that the catalytic sites are Pt metal particles attached

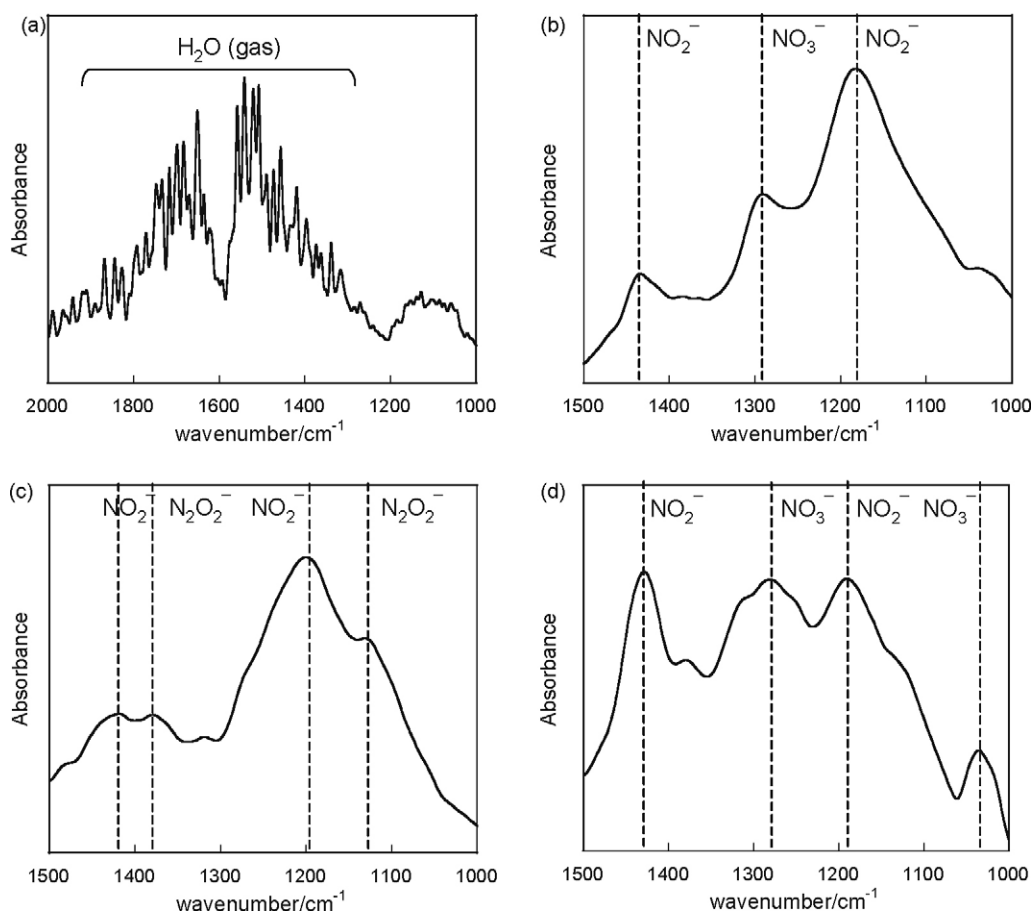


Fig. 8. DRIFT spectra observed on (a) the Pt metal particles prepared by the solvothermal method, (b) the sole CeO₂ with high surface area, (c) the catalyst prepared by physically mixing (a) and (b), and (d) ST-Pt/H-CeO₂.

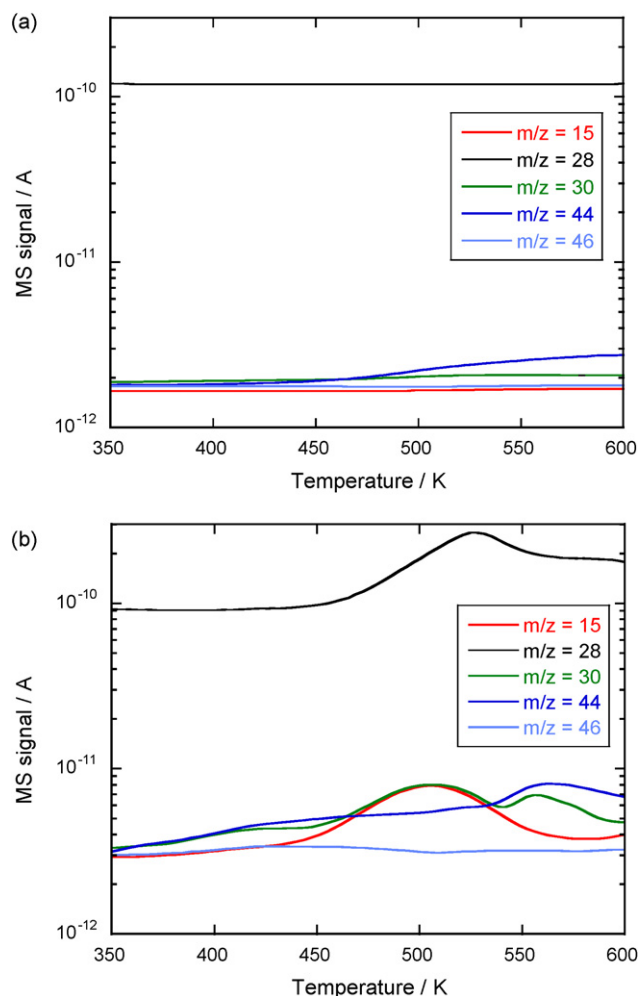


Fig. 9. H_2 temperature-programmed reaction profiles on (a) the sole Pt metal particles and (b) the Pt/ CeO_2 mixed catalyst. Before starting the reaction, the NO_x species were adsorbed on the catalyst surface by passing the $NO-O_2$ mixed gases at 473 K. Respective $m/z = 15, 28, 30, 44,$ and 46 are corresponded to $NH^+, N_2^+, NO^+, N_2O^+$, and NO_2^+ .

to the CeO_2 support which can serve as a NO_x reservoir. Fig. 8 (c) shows the DRIFT spectrum for the Pt/ CeO_2 mixed catalyst. No peak arose from nitrate ion could be detected. Strong transmission peak at 1200 cm^{-1} might be originated from nitrite ion and shoulder peaks at 1120 cm^{-1} and 1380 cm^{-1} is assigned to hyponitrite ion ($N_2O_2^{2-}$) [16]. This spectrum profile is somewhat different from the DRIFT spectrum reported previously in the $NO-H_2-O_2$ reaction system [20]. It has been proposed that NO_x transforms into N_2 by hydrogen attacking to NO_3^- ion species as observed on the DRIFT spectrum for ST-Pt/H- CeO_2 as shown in Fig. 8(d) [7]. Disappearance of NO_3^- peak implies that the reaction between intermediate NO_3^- and hydrogen is too fast to detect by the DRIFT spectroscopy and this behavior supposedly contributes to the N_2 selectivity. Further investigation is needed to elucidate the reaction mechanism in detail.

Next, effect of metal oxide supports on the NO_x conversion and N_2 selectivity was examined. The Pt/ Al_2O_3 ($123\text{ m}^2/\text{g}$), Pt/ ZrO_2 ($94\text{ m}^2/\text{g}$), and Pt/ TiO_2 ($73\text{ m}^2/\text{g}$) catalysts were prepared by physically mixing the Pt metal particles (1 wt%) with each support supplied from the Catalysis Society of Japan as JRC-ALO-3, JRC-TIO-1, and JRC-ZRO-3, respectively. These catalysts resulted in the almost same catalytic activity with the NO_x conversion of 70–80% and N_2 selectivity of 20–35%. The Pt/ CeO_2 mixed catalyst provided the superior NO_x reduction ability compared to other catalysts. The

solid basicity related to the NO_x adsorption is in the following order: $CeO_2 > ZrO_2 > Al_2O_3 > TiO_2$ [21,22]. It is considered that the adsorption site with certain degree of basicity contributes to enhance the N_2 selectivity by condensing the intermediate NO_3^- species. Moreover, the influence of the Pt metal particles on the NO_x reducing properties was investigated. The Pt metal particles were precipitated by refluxing 200 ml of a $Pt(NO_3)_2$ ethylene glycol solution (1 mM) at 470 K for 3 h. The solution color changed from yellow to black during the reaction, and the fine black powders were separately obtained by centrifuging the resultant product. The Pt metal particles prepared from the reflux method formed in a rectangular shape as shown in Fig. 6(b). Fig. 5(d) shows the NO_x conversion on a catalyst by mixing the Pt particles (reflux method) with the CeO_2 support (high surface area). The highest N_2 selectivity of 75% was observed with relative high NO_x conversion (ca. 80%). This result suggests that nature of the metal particles more influences on the NO_x reduction activity than the support. Although both XRD patterns for the Pt particles prepared by the solvothermal and the reflux methods were assigned to a fcc Pt metal phase, their particle morphology was distinct as shown in Fig. 6. Balint et al. reported that the facet effect on Pt metal plays an important role in NO dissociation and controls the reaction selectivity to N_2 and N_2O in the $NO-C_3H_6-O_2$ reaction system [23,24]. The rectangular shape observed on the Pt particles prepared by the solvothermal method indicates the anisotropic crystal growth along a specific plane. Such specific facet exposed on the Pt particles may be responsible for the high N_2 selectivity.

4. Conclusions

The NO_x reduction activity on the Pt supported ceria catalysts was examined. The NO_x reduction activity is significantly affected by the physicochemical characteristic of the metal-support interface and the best catalytic activity has been, consequently, obtained on the Pt/ CeO_2 catalyst prepared by physically mixing the Pt metal particles and the CeO_2 support where the contact force, namely, metal-support interaction has been moderately reduced. The DRIFT spectra indicate that the relevant intermediate adsorption species is NO_3^- and fast hydrogenation to it may leads the high N_2 selectivity. The high performance de NO_x catalyst can be designed by selecting the supports with suitable basicity and the metal with high affinity against NO, H_2 , and O_2 dissociation.

Acknowledgements

This work was partly supported by a Grant-in-Aid for Scientific Research on Priority Area A of “Panoscopic Assembling and High Ordered Functions for Rare Earth Materials” from the Ministry of Education, Culture, Sports, Science, and Technology.

References

- [1] M. Iwamoto, H. Yahiro, Y. Ta-u, S. Sundo, N. Mizuno, *Shokubai* 32 (1990) 430–433.
- [2] R. Burch, P.J. Millington, A.P. Walker, *Appl. Catal. B: Environ.* 4 (1994) 65–94.
- [3] K. Sakurai, Y. Okamoto, T. Imanaka, S. Teranishi, *Bull. Chem. Soc. Jpn.* 49 (1976) 1732–1735.
- [4] M. Markvart, V.L. Pour, *J. Catal.* 7 (1967) 279–281.
- [5] M. Koebel, M. Elsener, T. Marti, *Combust. Sci. Technol.* 121 (1996) 85–102.
- [6] K. Shimizu, A. Satsuma, *Appl. Catal. B: Environ.* 77 (2007) 202–205.
- [7] M. Machida, S. Ikeda, *J. Catal.* 227 (2004) 53–59.
- [8] C.N. Costa, P.G. Savva, J.L.G. Fierro, A.M. Efstathiou, *Appl. Catal. B: Environ.* 75 (2007) 147–156.
- [9] A. Abu-Jrai, A. Tsolakis, A. Megaritis, *Int. J. Hydrogen Energy* 32 (2007) 3565–3571.
- [10] M. Machida, S. Ikeda, D. Kurogi, T. Kijima, *Appl. Catal. B: Environ.* 52 (2004) 281–286.
- [11] M. Itoh, M. Saito, K. Motoki, J. Iwamoto, K. Machida, in preparation.
- [12] M. Itoh, N. Tajima, M. Saito, J. Iwamoto, K. Machida, in preparation.
- [13] R.F. Hicks, Q.J. Yen, A. Bell, *J. Catal.* 89 (1984) 498–510.

- [14] M. Machida, S. Ikeda, D. Kurogi, T. Kijima, *Appl. Catal. B: Environ.* 35 (2001) 107–116.
- [15] W. Khaodee, B. Jongsomjit, S. Assabumrungrat, P. Praserttham, S. Goto, *Catal. Commun.* 8 (2007) 548–556.
- [16] S. Philipp, A. Drochner, J. Kunert, H. Vogel, J. Theis, E.S. Lox, *Top. Catal.* 30 (31) (2004) 235–238.
- [17] A. Martinez-Arias, J. Soria, J.C. Conesa, X.L. Seoane, A. Arcoya, R. Cataluna, *J. Chem. Soc., Faraday Trans.* 91 (1995) 1679–1688.
- [18] A. Ueda, T. Nakao, M. Azuma, T. Kobayashi, *Catal. Today* 45 (1998) 135–138.
- [19] N. Macleod, R.M. Lambert, *Appl. Catal. B: Environ.* 35 (2002) 269–279.
- [20] M. Machida, M. Uto, D. Kurogi, T. Kijima, *J. Mater. Chem.* 11 (2001) 900–904.
- [21] A.L. Petre, A. Auroux, P. Célin, M. Calderaru, N.I. Ionescu, *Thermochim. Acta* 379 (2001) 177–185.
- [22] D. Martin, D. Duprez, *J. Phys. Chem.* 100 (1996) 9429–9438.
- [23] I. Balint, A. Miyazaki, K. Aika, *Phys. Chem. Chem. Phys.* 6 (2004) 2000–2002.
- [24] B. Ioan, A. Miyazaki, K. Aika, *Appl. Catal. B: Environ.* 59 (2005) 71–80.